Stretch-Induced Mitogen-Activated Protein Kinase Activation in Lung Fibroblasts Is Independent of Receptor Tyrosine Kinases

Francis Boudreault[1] and Daniel J. Tschumperlin[1]

[1]Molecular and Integrative Physiological Sciences Program, Department of Environmental Health, Harvard School of Public Health, Boston, Massachusetts

Lung growth and remodeling are modulated by mechanical stress, with fibroblasts thought to play a leading role. Little mechanistic information is available about how lung fibroblasts respond to mechanical stress. We exposed cultured lung fibroblasts to tonic stretch and measured changes in phosphorylation status of mitogen-activated protein kinases (MAPKs), selected receptor tyrosine kinases (RTKs), and phospholipase Cγ1 (PLCγ1) and activation of the small G-protein Ras. Human lung fibroblasts (LFs) were seeded on matrix-coated silicone membranes and exposed to equibiaxial 10 to 40% static stretch or 20% contraction. LFs were stimulated with EGF, FGF2, or PDGF-BB or exposed to stretch in the presence of inhibitors of EGFR (AG1478), FGFR (PD173074), and PDGFR (AG1296). Phospho-MAPK, phospho-RTK, and phospho-PLCγ1 levels were measured by Western blotting. Active GTP-Ras was quantified by immunoblotting after pull-down with a glutathione S-transferase–Raf-RBD construct. Normalized p-ERK1/2, p-JNK, and p-p38 levels increased after stretch but not contraction. Ligands to RTKs broadly stimulated MAPKs, with the responses to EGF and PDGF most similar to stretch in terms of magnitude and rank order of MAPK responses. Stretching cells failed to elicit measurable activation of EGFR, FGFR (FRS2α phosphorylation), or PDGFR. Potent inhibitors of the kinase activity of each receptor failed to attenuate stretch-induced MAPK activation. PLCγ1 and Ras, prominent effectors downstream of RTKs, were not activated by stretch. Our findings demonstrate that MAPKs are potently activated by stretch in lung fibroblasts, but, in contrast to stress responses observed in other cell types, RTKs are not necessary for stretch-induced MAPK activation in LFs.

Keywords: mechanotransduction; MAPK; EGFR; FGFR; PDGFR

CLINICAL RELEVANCE

Lung inflation and stretch act as powerful stimuli for growth, but the mechanisms remain poorly understood. Lung fibroblasts respond to tonic stretch with potent activation of mitogen-activated protein kinase signaling pathways but do so independently of receptor tyrosine kinases and Ras, distinguishing their stretch response from mechanotransduction in other cell types.

The lungs exhibit remarkable sensitivity to stretch. Occluding the trachea during fetal growth, a maneuver that increases intraluminal pressure and stretches the developing lung, results in accelerated development and increased airways branching (1). On the other hand, conditions that deflate or contract the developing lung and reduce stretch result in lung hypoplasia (2, 3). Postnatally, lung growth is stimulated by the stretch that accompanies enlargement of the thoracic cavity, directing lung growth proportional to the changes in size and shape of the surrounding environment (4). Stretch also serves as a potent stimulus for regeneration of lung tissue post-pneumonectomy (5, 6). It remains largely unexplained, however, how mechanical stretch coordinates and promotes lung growth. Lung fibroblasts (LFs) are known to play major roles in matrix synthesis, tissue remodeling, and lung development (3), and evidence points to their early proliferation (7) and activation after tracheal ligation–induced stretch in the fetal lung (8), but little is known about the early signaling responses of lung fibroblasts to stretch and contraction.

Tissue growth and regeneration are complex processes that require, among other events, coordinated cellular proliferation and differentiation. The mitogen-activated protein kinases (MAPKs) play pivotal roles in these processes. The prototypical activators of ERK1/2 (p44/p42) are growth factors, whereas JNK1/2/3 and p38 are typically stimulated by environmental stresses and inflammatory cytokines (9, 10). In general, p38 responses overlap with JNK responses and promote cell differentiation, migration, and apoptosis, whereas ERK is typically implicated in cell growth and proliferation (11). Although MAPKs are known to be activated when cells are mechanically stretched (12), the mechanisms of MAPK activation by stretch are debated and may differ in a cell-specific manner.

The current consensus view of MAPK activation by mechanical stretch involves upstream activation of putative cell surface mechanoreceptors or intracellular mechanosensors (12, 13). Receptor tyrosine kinases (RTKs) have been proposed as mechanoreceptors in a variety of contexts. RTKs are single transmembrane domain cell surface receptors found only in multicellular animals. The human genome contains 20 families of RTKs encoded by 58 genes (14). In the lung, fibroblast growth factor receptor-2b (FGFR2b) and the platelet-derived growth factor (PDGFR) have been implicated in stretch-induced lung growth *in utero* (1, 15), and the epidermal growth factor receptor (EGFR) has been shown to mediate stretch-induced alveolar type II cell differentiation (16). The latter study demonstrated that cyclic stretch-induced ERK1/2 phosphorylation was blocked by an EGFR inhibitor and that stretch stimulated EGFR phosphorylation and Ras activation, strongly implicating EGFR in lung epithelial responses to stretch. In a similar study, EGFR was found to be involved in cyclic stretch activation of ERK1/2, although Ras was not implicated (17). The mechanoactivated nature of RTKs has been observed in other tissues as well: Mechanical stretch activates EGFR in keratinocytes (18), stimulates proliferation of vascular smooth muscle cells via the insulin-like growth factor receptor (19), and activates the EGFR (20) and the PDGFR (21, 22), with the

(*Received in original form March 12, 2009 and in final form June 25, 2009*)

This work was supported by National Institutes of Health grant R01 HL-082856.

Correspondence and requests for reprints should be addressed to Daniel J. Tschumperlin, Ph.D., Department of Environmental Health, Harvard School of Public Health, 665 Huntington Ave, Boston, MA 02115. E-mail: dtschump@hsph.harvard.edu

Am J Respir Cell Mol Biol Vol 43. pp 64–73, 2010
Originally Published in Press as DOI: 10.1165/rcmb.2009-0092OC on August 14, 2009
Internet address: www.atsjournals.org

latter implicated in mechanical strain-induced embryonic stem cell differentiation into vascular smooth muscle cells (23). In this study, we focused on whether the receptor tyrosine kinases EGFR, FGFR, and PDGFR play roles in the proximal mechanotransduction response of human lung fibroblasts to tonic stretch.

MATERIALS AND METHODS

Reagents and Antibodies

DL-Dithiothreitol (DTT), sodium orthovanadate, and sodium fluoride were obtained from Sigma (St. Louis, MO). RTK inhibitors AG1478, PD173074, and AG1296 were purchased from EMD/Calbiochem (Carlsbad, CA) and dissolved in DMSO. Recombinant human EGF, FGF2, and PDGF-BB were from Cell Signaling Technology (Danvers, MA). Rabbit polyclonal anti-ERK1/2, anti-phospho-ERK1/2 (Thr202/Tyr204) pAb, anti-p38α/β/γ, anti-phospho-p38α/β/γ (Thr180/Tyr182) mAb, anti-SAPK/JNK1,2,3 mAb, anti-phospho-SAPK/JNK1,2,3 (Thr183/Tyr185) pAb, anti-phospho-EGF receptor (Tyr1068) pAb, anti-phospho-FRS2α (Tyr196) pAb, anti-phospho-PDGFRα (Tyr849)/PDGFRβ (Tyr857) mAb, anti-phospho-PLCγ1 (Tyr783) pAb, anti-phospho tyrosine mAb (p-Tyr-102), goat anti-rabbit IgG horseradish peroxidase (HRP)-linked Ab, and anti-biotin HRP-linked were from Cell Signaling Technology. Goat anti-β-actin pAb and rabbit anti-goat IgG HRP-conjugated were from Santa Cruz Biotechnology (Santa Cruz, CA).

Cells

Human juvenile (5-yr-old donor) lung fibroblasts CCL-151 and human fetal lung fibroblasts CCL-153 (ATCC, Manassas, VA) were grown in F12K medium (ATCC) supplemented with 10% FBS (Lonza, Basel, Switzerland), 100 IU/ml penicillin, and 100 μg/ml streptomycin (Mediatech Inc., Herndon, VA).

Stretch–Contraction Device

The design of the stretch–contraction device (Figures 1A and 1B) was modified from a previously described apparatus (24). It consists of a 6-well BioFlex plate (FlexCell, Hillborough, NC) secured tightly with six flat-head screws on an aluminum sliding platform. The fixation screws allow the cover to remain in place without hindering the flow of air. The movement of the sliding platform is stabilized by four rods fitted inside Teflon bushings. The platform rests on four springs, which prevent the 6-well BioFlex plate from making contact with the posts before application of the stretch and provide smooth and regular displacement of the platform. The platform is lowered manually by screwing down a pair of phenolic three-arm knobs to stretch the silicon substrate. As the plate moves downward, the silicon membrane stretches over the 28.6-mm-diameter Teflon post coated with a thin layer of high vacuum grease (Dow Corning, Midland, MI) (Figure 1C). The plate displacement is measured with a digital caliper (Mitutoyo, Kawasaki, Japan). The relationship between the displacement of the plate and the level of substrate strain was validated by video imaging (Figure 1D). Five square-shaped marks of approximately 10 mm^2 were drawn with an indelible marker on the membrane. Linear strain was calculated from measured changes in area at different plate displacements. The range of applicable strain is −30 to +40%. Indentor posts are removeable so that unstretched control wells can be included on each plate as desired.

A unique attribute of this device is the ability to culture cells on prestretched membranes for extended periods and study responses subsequent to substrate contraction. For contraction experiments, cells were seeded in prestretched wells that contained a "seeding ring" with internal diameter of 20 mm to restrict the cell seeding area over the indentor post (Figure 1C). The seeding ring is made of machined biomedical-grade nylon 6,6 with a stainless steel handle, a Buna-N O-ring 1.5 mm width to squeeze the ring tight inside the well, and a 0.5-mm-thick silicon gasket on the bottom to block fluid leakage. The ring, removed 24 hours after seeding, prevented cells from attaching to the periphery of the substrate surface beyond the dimensions of the underlying indentor.

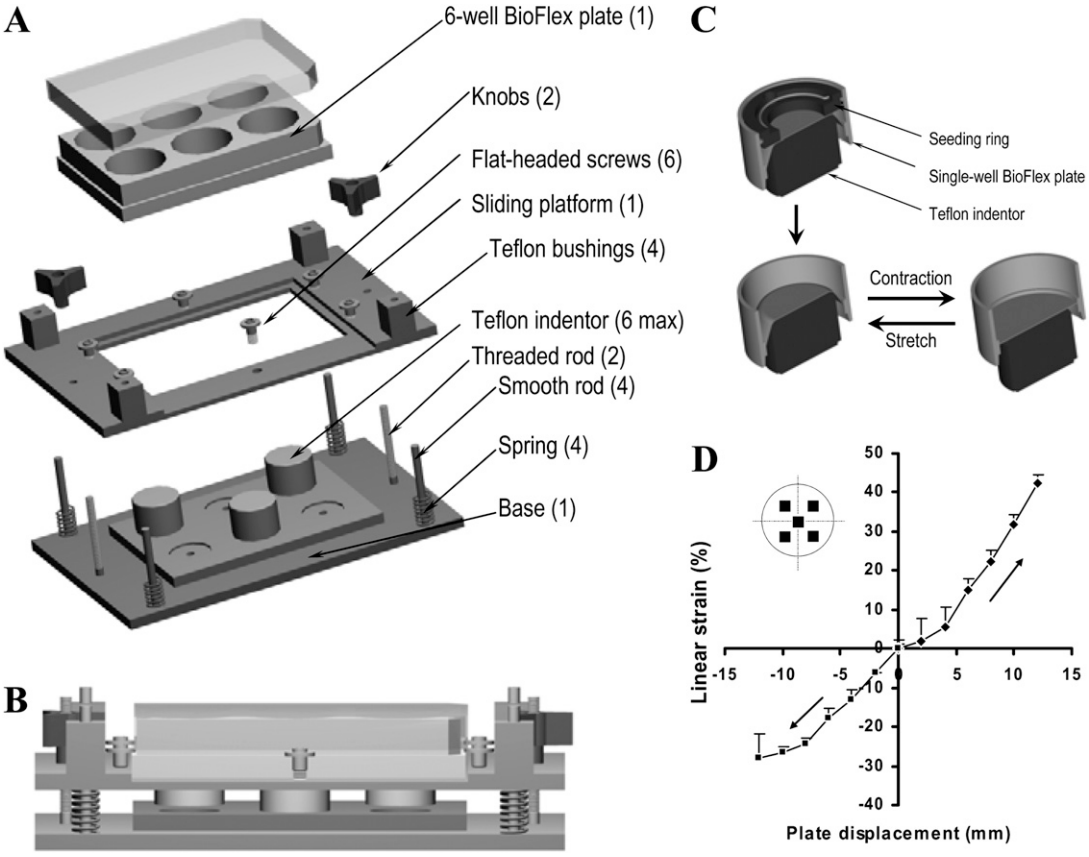

Figure 1. Description and validation of the stretch–contraction device. (*A*) Assembly of the stretch–contraction device. Teflon indentor posts are positioned beneath each well to be strained. In the configuration shown here, three wells (out of a total of six wells) are left unstretched for control measurement (quantity in parentheses). (*B*) Side view of the stretch–contraction device assembled with a BioFlex plate. (*C*) Single-well cross sections describing contraction and stretch. (*D*) Changes in linear strain relative to plate displacement assessed by measuring with video microscopy the relative deformation of markers (*inset*) drawn on the flexible silicon membrane.

Stretch, Contraction, and Growth Factor Stimulation Experiments

Cells were seeded on collagen I–coated BioFlex plates (FlexCell) at 20,000 cells/cm^2 in 10% FBS-supplemented medium for 24 hours and serum starved for a subsequent 24 hours. In some experiments, cells were seeded in an identical manner on pronectin- or laminin-coated Bioflex plates. Under such growth conditions, cells covered approximately 75 to 90% of the membrane at the time of experiment, and cell density was similar to seeding level as measured in separate experiments (data not shown). Cells were subjected to equibiaxial stretch or contraction and held strained at 37°C and 5% CO_2 until time of lysis. Growth factors were added to the wells as described for each experiment. For each receptor, we selected the agonist that maximizes the chance of activating one or more of the isoforms expressed by LFs: FGF2, EGF, and PDGF-BB. Four genes belong to the FGFR family (*FGFR1–4*), but up to 15 variants arising from alternative gene splicing are expressed. FGF2 (basic FGF) binds to all four FGFR isoforms (25). EGFR, a member of the HER/ErbB family of receptors, is encoded by only one gene but can bind numerous growth factors, including EGF (26). PDGFR exists in two isoforms that are the product of two separate genes. Four ligands for this receptor, PDGFA-Ds have been described that form homo- and heterodimers. The PDGF-BB homodimer used here binds PDGFRα and PDGFRβ (27).

Immunoblot Analysis

Cells were washed twice with ice-cold PBS and lysed in 150 μL Laemmli sample buffer 62.5 mM Tris-HCl (pH 6.8); 25% glycerol; 2% SDS; 0.01% Bromophenol blue (Bio-Rad, Hercules, CA) containing 50 mM DTT; 100 μM sodium orthovanadate; and 10 mM sodium fluoride. For MAPK assay, proteins were resolved by electrophoresis on 10% Tris-HCl polyacrylamide gel (Bio-Rad) in SDS-Tris buffer and transferred to a 0.2-μm nitrocellulose membrane for 1 hour at 100 V in Tris buffer with 20% methanol. For RTKs, PLCγ1, and phosphotyrosine assay, proteins were resolved by electrophoresis on 7.5% Tris-HCl polyacrylamide gel (Bio-Rad) in SDS-Tris buffer and transferred to a 0.2-μm PVDF membrane for 1 hour at 100 V in Tris buffer without methanol. Membranes were blocked with 5% wt/vol fat-free milk and probed overnight at 4°C with primary antibodies diluted in TBS-T (Tris buffered saline [pH 7.6], 0.1% Tween 20) containing 5% wt/vol BSA. The blots were probed with horseradish peroxidase–conjugated secondary antibody for 1 hour at room temperature (RT). Bands were visualized with enhanced chemiluminescent reagent (Pierce, Rockford, IL) and quantified with digital imaging and densitometry analysis. The magnitude of phospho-MAPK responses was normalized to total (phospho+unphospho) measured on separate blots. Unless otherwise described, each MAPK fold-change was calculated relative to unstimulated time-matched control samples.

PDGFRβ Immunostaining

Cells washed twice with ice-cold PBS were fixed with Formalin 1:10 dilution (10% formaldehyde phosphate-buffered; Fischer Scientific, Kalamazoo, MI) for 10 minutes and blocked with 5% goat serum for 30 minutes at RT. The fixed cells were incubated with primary Ab anti-PDGFRβ (Cell Signaling Technology) at 4°C on rocking platform and incubated with secondary antibody (Texas Red goat anti-rabbit IgG [H+L] conjugated; Invitrogen, Carlsbad, CA) for 1 hour at RT. Images were visualized with fluorescence-equipped NIKON 200 TE microscope (Nikon, Japan) and acquired with computer-controlled digital camera.

Active Ras Pull-Down Assay

Ras activation was analyzed using the EZ-Detect Ras Activation Kit (Pierce) as described by the manufacturer. Cells were washed twice with PBS and lysed with 25 mM Tris-HCl (pH 7.5), 150 mM NaCl, 5 mM $MgCl_2$, 1% NP-40, 1 mM DTT, and 5% glycerol. Cell lysates were centrifuged for 15 minutes at 16,000 × *g* at 4°C, and the supernatant was collected. A small fraction was kept for total Ras content analysis. Activated GTP-bound Ras was pulled down with a glutathione S-transferase–Raf1-RBD (Ras binding domain) construct immobilized on a glutathione gel. Eluates were mixed 1:1 with SDS sample buffer, 125 mM Tris-HCl (pH 6.8), 2% glycerol, 4% SDS (wt/vol), and 0.05% bromophenol blue, separated on 15% Tris-HCL polyacrylamide gel by electrophoresis, and transferred to a 0.2-μm PVDF membrane. The membrane was probed with mouse monoclonal $Ig_{2a}\kappa$ anti-Ras antibody and with horse anti-mouse IgG (H&L) HRP-conjugated Ab (Cell Signaling Technology). Immunoblots were imaged as described above.

Statistical Analysis

Data are shown as mean ± SD. Statistical comparisons were made using paired Student's *t* test. $^*P < 0.05$; $^{**}P < 0.01$; $^{***}P < 0.001$.

RESULTS

Tonic Stretch Activates MAPKs in Lung Fibroblasts

We first tested whether the phosphorylation level of MAPKs change when juvenile lung fibroblasts (CCL-151) are tonically stretched or contracted. CCL-151 cells were grown for 2 days on collagen I–coated silicon membranes and stretched by 25% or contracted by −20% (an equivalent displacement from starting conditions) for 10 minutes. Protein phosphorylation, an indicator of MAPK activation status, was significantly increased by stretch in all three MAPKs we examined (ERK, JNK, and p38), but the magnitude of the response varied (Figure 2A). The relative fold-change was similar within the MAPK isoforms (ERK1 versus ERK2 and JNK1 versus JNK2/3); therefore, the individual isoform responses were merged and reported as a single value. The largest response to tonic stretch was in the p38 pathway. We did not detect any significant response to contraction (negative strain) for any of the MAPKs. Similar findings were obtained with fetal-derived CCL-153 lung fibroblasts (Figure 2B), emphasizing that MAPK responses to stretch are largely preserved across fetal- and juvenile-derived lung fibroblasts. For the remainder of this study, only the CCL-151 lung fibroblasts were tested.

MAPK Activation Is Transient and Strain Dependent

We examined whether the nature of the substrate matrix coating modulates the MAPK response to stretch. Cells grown on pronectin (fibronectin-like RGD binding site), laminin, or collagen I exhibited strikingly similar MAPK responses to stretch (Figure 3A). Because laminin is bound mainly by $\alpha_6\beta_1$ integrins, pronectin by $\alpha_5\beta_1$, and collagen I by $\alpha_1\beta_1$ and $\alpha_2\beta_1$, these results suggest that the MAPK responses to stretch are largely independent of the identity of the α integrin subunit involved in matrix binding. In preliminary experiments, stretch also failed to stimulate phosphorylation of focal-adhesion kinase on Tyr925 (data not shown), suggesting that the MAPK response to stretch was not downstream of integrin/focal adhesion kinase signaling.

We next examined the time-course of MAPK activation by tonic stretch (25%) over a period of 2 hours (Figure 3B). MAPK phosphorylation levels transiently increased at similar relative rates for all three MAPKs (peak between 10 and 30 min) and returned to near baseline values 120 minutes after the start of tonic stretch. The transient nature of MAPK activation by tonic stretch is not atypical because cells stimulated by various growth factors, proinflammatory cytokines, or ligands for G protein–coupled receptors exhibit similar transient MAPK activation (28–31). Cyclic stretch (17, 20, 32) and a variety of other physical stimuli, such as abrupt temperature changes (33), also result in transient MAPK activation. Not all MAPK activation is transient, however, because a slower but more sustained response is sometimes observed in response to stimuli such as UV exposure (34), hypertonic shock (31), and TGF-β1 (35).

Although mechanical stretch is known to promote lung growth, large stretch magnitudes can also contribute to cellular

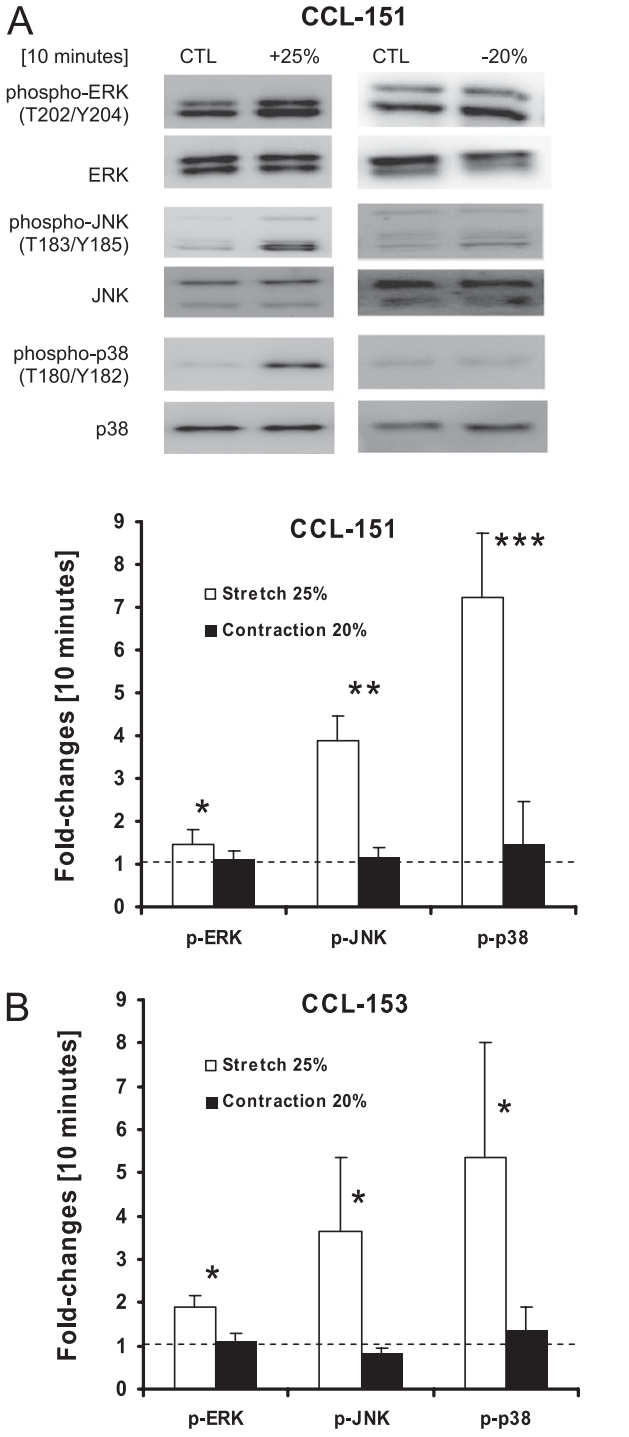

Figure 2. Mitogen-activated protein kinase (MAPK) activation by tonic stretch in lung fibroblasts (LFs). (*A, top*) Tonic stretch enhances phosphorylation of ERK1/2, JNK1/2/3, and p38 in CCL-151 juvenile lung fibroblasts. Strain was gradually applied over approximately 50 seconds. Cells were kept stretched (25%) or contracted (−20%) for 10 minutes. Representative blots of three experiments are shown. CTL = control. (*Bottom*) Fold-change in phosphorylated MAPK levels induced by strain compared with time-matched unstrained cells (n = 3). (*B*) Fetal LFs MAPK responses are similar to juvenile LFs. CCL-153 fetal LFs were assayed as described in *A* and analyzed for MAPK activation (n = 3).

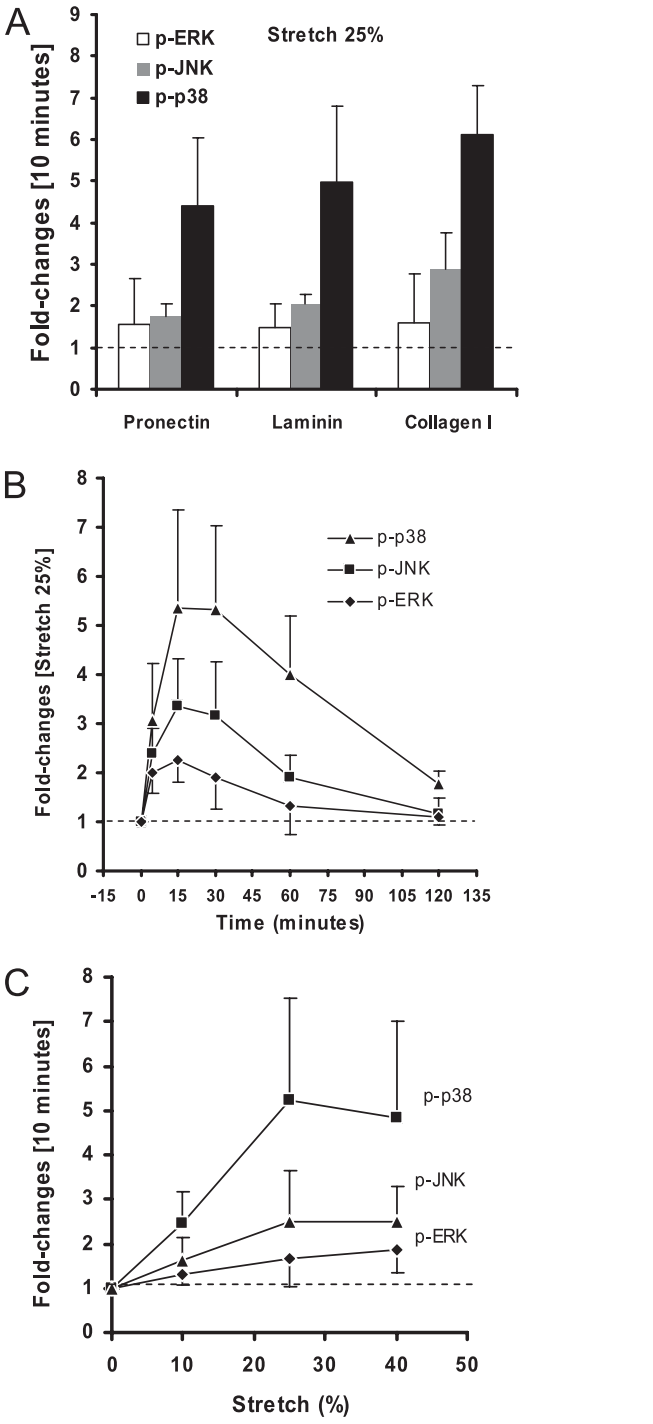

Figure 3. Characterization of MAPK activation by tonic stretch in LFs. (*A*) Matrix coating has little effect on MAPK stimulation. CCL-151 were grown on pronectin-, laminin-, or collagen I–coated substrates and subjected to 25% stretch and analyzed for MAPK activity (n = 3). (*B*) Stretch transiently enhances MAPK activation in lung fibroblasts. Cells were tonically 25% stretched for increasing periods of time before lysis and MAPK analysis. An independent 6-well BioFlex plate was used for each time increment (n = 3 per increment). (*C*) Cells were stretched with amplitudes of 10, 25, and 40% and assessed for MAPK phosphorylation. Each strain increment is measured from an independent 6-well BioFlex plate (n = 3 per increment).

injury (36, 37). Therefore, we tested whether MAPKs were activated proportionally to the amount of stretch applied or exhibited differential sensitivity to stretch magnitude. Activation of each MAPK family by tonic stretch in LFs increased monotonically with increasing magnitude of applied strain below 25% and showed signs of reaching a plateau when

approaching 40% (Figure 3C). This maximum strain magnitude was chosen because *in vivo* LFs reside in airways and parenchyma, which can experience similar magnitude strains (38).

MAPK Activation by Growth Factors in LFs

To explore the possible role for RTK activation in stretch-induced MAPK activation, we first measured changes in MAPK phosphorylation when cells were stimulated with ligands to FGFR, EGFR, and PDGFR. Similar to stretch/contraction experiments, we examined MAPK activation after stimulating cells for 10 minutes. This time point was selected because in pilot experiments (not shown) the ERK response to FGF2 exhibited kinetics of activation very similar to 25% stretch during the first 1 hour (peak ~10–15 min).

With the exception of p38, which was poorly stimulated by FGF2, we found that each growth factor enhanced MAPK activation with magnitude similar to 25% stretch (Figure 4). These results confirmed that LFs express functional EGFR, FGFR, and PDGFR. Based on the known downstream links of these RTKs to MAPKs, we suspected that PDGFR or EGFR alone or in combination with FGFR might play a role in mediating stretch-induced MAPK activation.

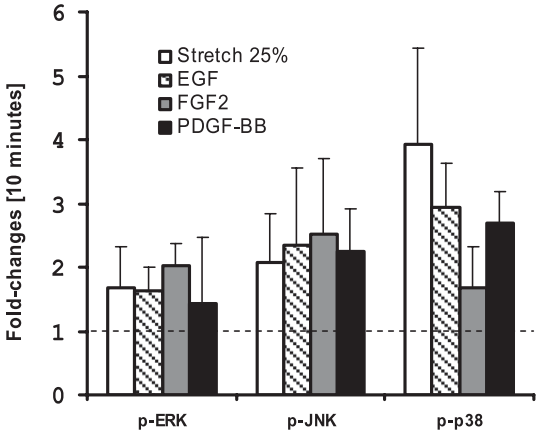

Figure 4. Growth factors activate MAPKs in CCL-151. At time zero, a volume equal to that already bathing the cells was added with EGF, FGF2 (basic FGF), or PDGF-BB at twice the final concentration of 100 ng/mL (three wells per plate). Untreated wells (three wells per plate) received an equal amount of fluid. Cell lysates were collected for analysis of MAPK phosphorylation.

EGFR, FGFR, and PDGFR Are Not Activated by Stretch in LFs

To test whether the RTKs EGFR, FGFR, and PDGFR are activated by stretch, we measured the extent of phosphorylation of specific residues on the cytoplasmic tail of each receptor. Although strong-affinity antibodies exist for phospho-EGFR and phospho-PDGFR, none could be found for FGFR. As a surrogate, we evaluated phosphorylation of FRS2α, a docking protein that associates with and is phosphorylated by FGFR (39). Phosphorylation of FRS2α by activated FGFR leads to the formation of Grb2/Sos complexes and downstream ERK1/2 activation.

Contrary to our expectations, application of 40% stretch to LFs, a level of strain able to activate ERK1/2 close to maximal exogenous ligand stimulation, failed to induce phosphorylation of EGFR, FRS2α, or PDGFR (Figure 5). In comparison, ligand-stimulation evoked prominent increases in tyrosine phosphorylation of all three receptor or receptor substrates. To further rule out stretch-induced signaling through PDGFR, which can activate ERK through an atypical mechanism that is independent of PDGFRβ-receptor tyrosine phosphorylation (40), we examined PDGFR clustering, a key signaling event indicative of RTK activation (41). Ligand-independent clustering of receptors has been reported for physical stimuli such as UV exposure and hypertonic shock (42). Although application of 100 ng/mL PDGF-BB for 15 minutes resulted in formation of punctuate PDGFRβ clusters that were absent in untreated control, no such receptor clustering could be detected within cells tonically stretched for the same period of time (Figure 6).

The findings shown in Figures 5 and 6 suggest that EGFR, FGFR, and PDGFR were unlikely to contribute to stretch-induced MAPK signaling, although a possibility remains that phosphorylation of alternative residues was involved in the mechanosensitive response. To more definitively rule out involvement of the selected RTKs, we pretreated cells with small-molecule inhibitors using concentrations known to block the kinase activity of each receptor: AG1478 (1 μM) for EGFR, PD173074 (1 μM) for FGFR, and AG1296 (10 μM) for PDGFR. If stretch uses a mechanosensor other than RTKs, these compounds should be ineffective in preventing MAPK activation by stretch. We chose ERK1/2 as our primary mechanoresponsive indicator because this MAPK was equally stimulated by all growth factors tested as well as by stretch (Figure 4). None of the RTK inhibitors significantly attenuated ERK1/2 activation by tonic stretch in lung fibroblasts (Figure 7), further reinforcing the conclusion that this trio of RTKs is not involved in proximal mechanotransduction in LFs. Similarly, we found that AG1478 and AG1296 failed to block 40% stretch-induced p38 and JNK activation (data not shown), suggesting more broadly that stretch activation of MAPKs in LFs is independent of EGFR and PDGFR. In addition, PD173074 did not suppress JNK activation by stretch; because stimulation with FGF did not effectively activate p38 (Figure 4), we did not test whether FGF receptor participates in stretch-induced p38 activation.

PLCγ1 Activation and Global Phosphotyrosine Responses to Stretch

To investigate more broadly whether the entire class of RTKs was stimulated by mechanical stretch, we first examined the activation of phospholipase C (PLC) by measuring phosphorylation of the PLCγ1 isoform. Although the 2-minute application of PDGF-BB strongly activated PLCγ1 in our cells, as measured by Tyr783 phosphorylation, 40% stretch for the same time period failed to induce a comparable change in PLCγ1 phosphorylation (Figure 8A). The observation that stretch-activated ERK1/2 was not attenuated by the aminosteroid PLC antagonist U-73122 corroborated this result (data not shown). Our results with human lung fibroblasts are thus clearly distinct from those obtained with fetal rat lung cells in which cyclic mechanical stretch stimulated herbimycin A–sensitive PLCγ1 phosphorylation (43). Based on this finding, we sought to determine whether MAPK activation in our cells was sensitive to the ansamycin antibiotic herbimycin A, a potent blocker of Src family protein kinases. Numerous RTKs, including EGFR and PDGRF, are known substrates for the nonreceptor tyrosine kinase c-Src (44), a signaling protein frequently shown to be activated by mechanical stress (43). In our experiments, herbimycin A failed to block stretch-induced MAPK in LFs (data not shown).

To further extend our investigation of RTK activation, we examined total protein tyrosine phosphorylation by Western blotting using an antibody able to recognize phosphorylated tyrosine residues independent of the identity of the surrounding amino acids. Once activated, RTKs are heavily tyrosine phosphorylated and thus became a target with multiple sites for the

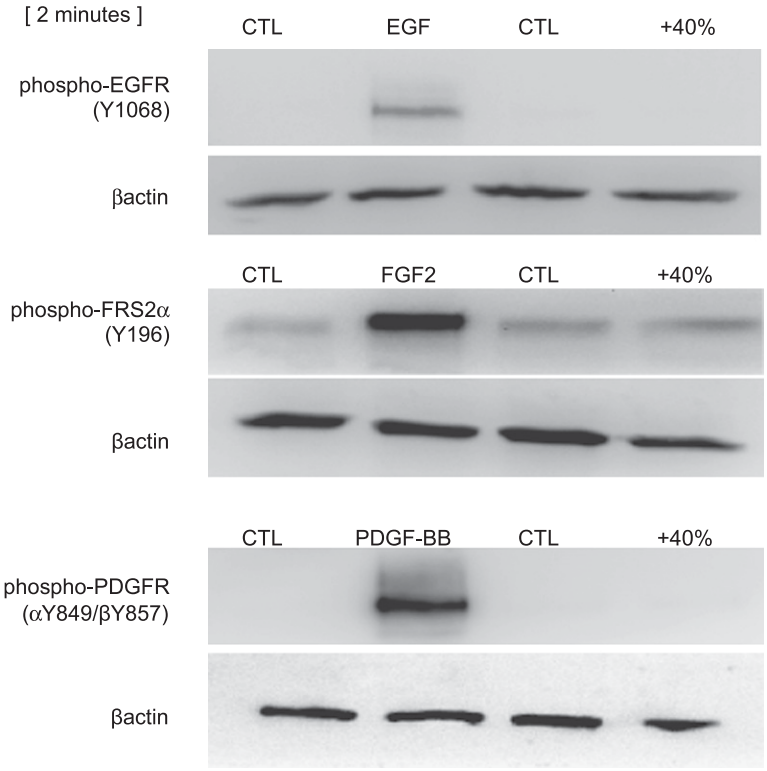

Figure 5. Stretch fails to activate receptor tyrosine kinases in LFs. CCL-151 were stimulated with growth factors (100 ng/ml) or stretched (40%) for 2 minutes. Lysates collected at the end of the treatment from individual wells were pooled (three treated and three untreated wells) to increase the protein level in each sample. Levels of tyrosine phosphorylation after treatments were visualized by immunoblotting. CTL = control. Representative blots are shown (n = 2).

phospho-tyrosine antibody. Furthermore, in the context of stretch-activated MAPKs, if RTKs are upstream in the signaling sequence, changes in their phosphorylation status should predominate at the earliest times after onset of stretch. As expected, the 2-minute application of ligands to EGFR, FGFR, and PDGFR enhanced tyrosine phosphorylation levels in the apparent molecular weight ranges associated with those receptors: EGFR (175 kD), FGFR (125 kD), and PDGFR (190 kD) (Figure 8B, *lanes 1–4*). However, the tyrosine phosphorylation profile of proteins collected from cells stretched 40% was indistinguishable from control (Figure 8B, *lane 5* compared with *lane 6*).

Ras Is Not Activated by 40% Stretch

A hallmark of ERK1/2 activation by RTKs is the involvement of the signaling molecule Ras, and we tested whether it was activated by stretch. Although the small GTPase Ras can be activated by RTK-independent mechanisms, the absence of Ras stimulation by stretch would further argue against RTK activation and involvement in stretch-induced MAPK stimulation.

Although the application of 100 ng/mL FGF2 to LFs resulted in a nearly 3-fold increase in GTP-bound Ras (Figure 8C), stretching lung fibroblasts by 40% failed to induce an increase in GTP-bound Ras (P = 0.43). Because we routinely observed that stretching LFs by 40% increases ERK1/2 phosphorylation similar to stimulation with 100 ng/ml FGF2, this strongly suggests that Ras is not involved in stretch-activated ERK1/2 in LFs. Because Ras activation is a cornerstone of ERK1/2 stimulation by RTKs, our findings confirm that the whole family of RTKs, including PDGFR, EGFR, and FGFR, do not contribute to stretch-induced MAPK activation in LFs.

DISCUSSION

Although fibroblasts play major roles in mechanically regulated lung development, remodeling, and regeneration, especially in the formation of new septa (45), their early responses to mechanical stretch have been less well studied than other constituent cells of the lung. In this study, the mechanosensitive nature of lung fibroblasts was demonstrated by robust activation of all three major MAPKs: ERK1/2, JNK1/2/3, and p38 by tonic stretch. We did not detect activation of any MAPK by contraction (−20%), suggesting a polarity in mechanical responsiveness that could help to explain the distinct growth and differentiation responses of fetal lung to stretch versus contraction/relaxation *in vivo* (7). We observed that application of 25% stretch stimulated MAPK activation to levels similar to saturating concentrations of EGF, FGF2, and PDGF-BB, which are known to be potent activators of MAPK signaling. Thus, the mechanosensitive responses of LFs are robust and comparable in magnitude

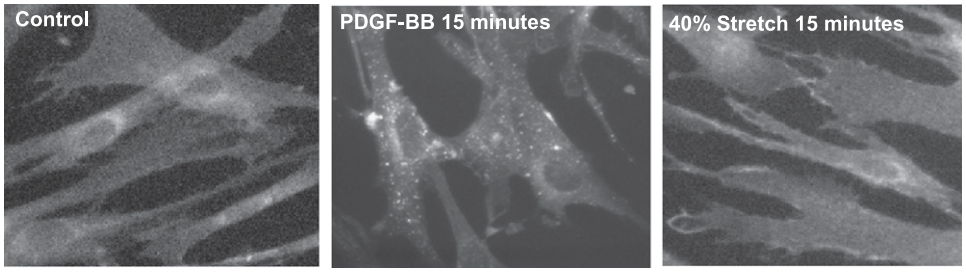

Figure 6. Stretch does not cluster PDGFRβ in CCL-151. Cells were stimulated with 100 ng/ml PDGF-BB or 40% tonic stretch for 15 minutes and fixed with 10% formaldehyde and immunoprobed for PDGFRβ as described in MATERIALS AND METHODS. Images are representative of similar results in two independent experiments.

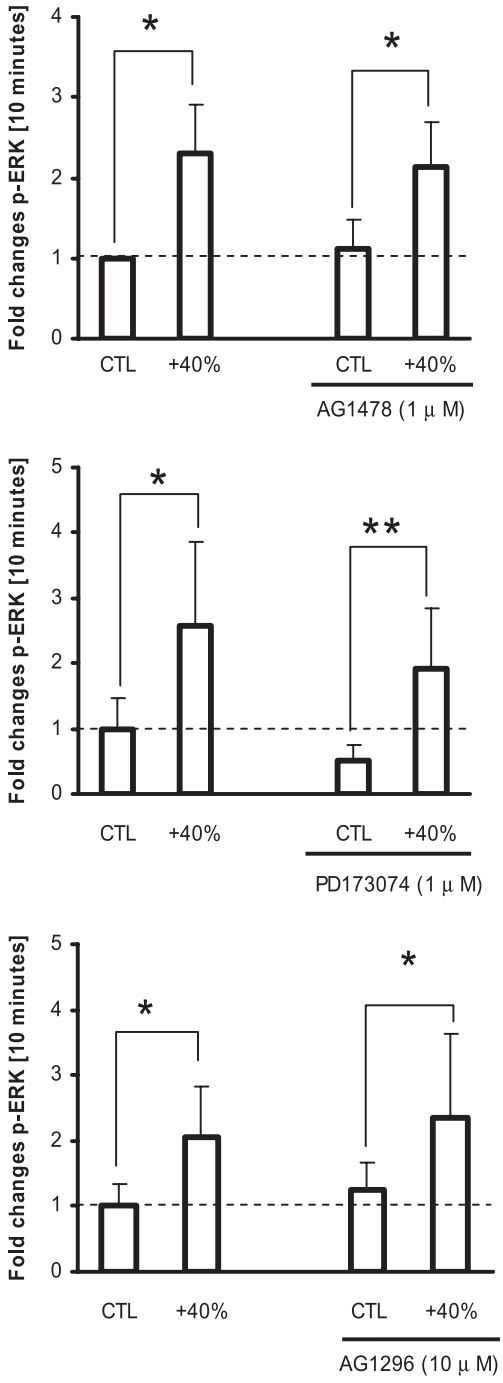

Figure 7. Stretch activates ERK despite inhibition of RTKs. CCL-151 were pretreated with selective kinase inhibitors for 5 minutes and stimulated with growth factors or 40% stretch for 10 minutes. For each inhibitor experiment, two 6-well BioFlex plates were used: control (two replicate wells), 40% (four replicate wells), control + inhibitor (two replicate wells), and 40%+inhibitor (four replicate wells). Cells were collected for ERK1/2 activation analysis. CTL = control.

to growth factor responses, reinforcing the likely importance of LF stretch-induced responses in lung biology.

Based on abundant evidence gathered from mechanical responses in other cell types, we hypothesized that lung fibroblasts respond to mechanical stretch through specific activation of receptor tyrosine kinases EGFR, FGFR, or PDGFR, leading to stretch-induced MAPK activation. Although the overall pattern of MAPK activation by mechanical stretch (p38 > JNK > ERK1/2) resembled the response to EGF and PDGF-BB stimulation, it appears that this similarity is coincidental because mechanical stretch failed to activate EGFR or PDGFR, and inhibition of those receptors did not attenuate the ERK1/2 response to stretch. Similarly, stretch did not activate FGFR, nor did a specific inhibitor of FGFR attenuate the ERK1/2 phosphorylation response to stretch, even though the magnitude of stretch applied (40%) elicited ERK1/2 phosphorylation to a level similar to saturating ligand concentrations (100 ng/ml). Given the strong responses of lung fibroblasts to ligands targeting these receptors, we conclude that although lung fibroblasts express functional PDGFR, EGFR, and FGFR, these receptors are not activated by stretch and therefore are not involved in stretch-induced MAPK activation.

Stretch also failed to increase activation of PLCγ1, a phospholipase isoform associated with numerous RTKs. The phosphoinositide-metabolizing enzymes PLCα, PLCβ, and PLCγ are major initiators of the inositol signaling pathway (46). In particular, the activation of PLCγ by RTK phosphorylation results in downstream activation of IP3-dependent intracellular Ca^{2+} signaling and PKC activation and regulation of ERK. PLCγ is known to be phosphorylated upon activation of a variety of RTKs, including EGFR, FGFR, and PDGFR as well as others, such as the hepatocyte growth factor receptor (Met) (47). Although RTKs are not the only type of receptor able to activate PLCγ (47), the absence of activation of PLCγ in our experiments further reduces the likelihood that RTKs as a class are activated by stretch in LFs. In addition, stretch failed to alter the content and distribution of tyrosine-phosporylated proteins in the high-molecular-weight range, which comprise many RTKs, measured shortly after the onset of stretch.

We analyzed the active state of the small GTPase membrane-associated Ras, an intermediate link between many RTKs and ERK1/2. Soon after stimulation of RTKs, guanodine nucleotide–releasing proteins, such as Sos, stimulate the inactive Ras to exchange its GDP for GTP. Active GTP-bound Ras binds to c-Raf kinase, the first link in the signaling cascade to ERK1/2 (48). Another well described signaling pathway to ERK by RTKs, the PLCγ pathway, relies on Ras (39). In our experiments, however, tonic stretch was ineffective in altering Ras activity levels in lung fibroblasts. This is striking considering how broadly Ras activation is implicated in ERK stimulation across a variety of signaling pathways (48). The failure of stretch to activate PLCγ1, the lack of detectable changes in protein tyrosine phosphorylation after stretch, and the absence of Ras activation by stretch strongly suggest that RTK-independent mechanisms link stretch to MAPK activation in LFs.

The absence of RTK mechanosensitivity in lung fibroblasts was surprising because the circumstantial case for their participation was well established. Indeed, several modes of activation of RTKs by physical stimulus have been identified. For instance, RTKs can be transactivated by GPCR-mediated increases in the rate of shedding of ligands for EGFR (49), a mechanism induced by osmotic shock in Cos-7 cells (50) and triggered by mechanical stretch in epithelial and vascular smooth muscle cells (17, 18, 22). Ligand-independent modes of activation of RTKs also exist. Mechanical challenges, such as an osmotic shock, can result in ligand-independent multimerization of EGFR (42) and PDGFR (51). In our experiments, none of these mechanisms appeared to be in play, indicating that RTKs do not contribute as primary sensors of mechanical stress in the lung fibroblast stretch response.

By ruling out RTK-dependent proximal mechanotransduction in LFs, our results serve to focus future investigations on candidate RTK-independent mechanosensitive pathways, in-

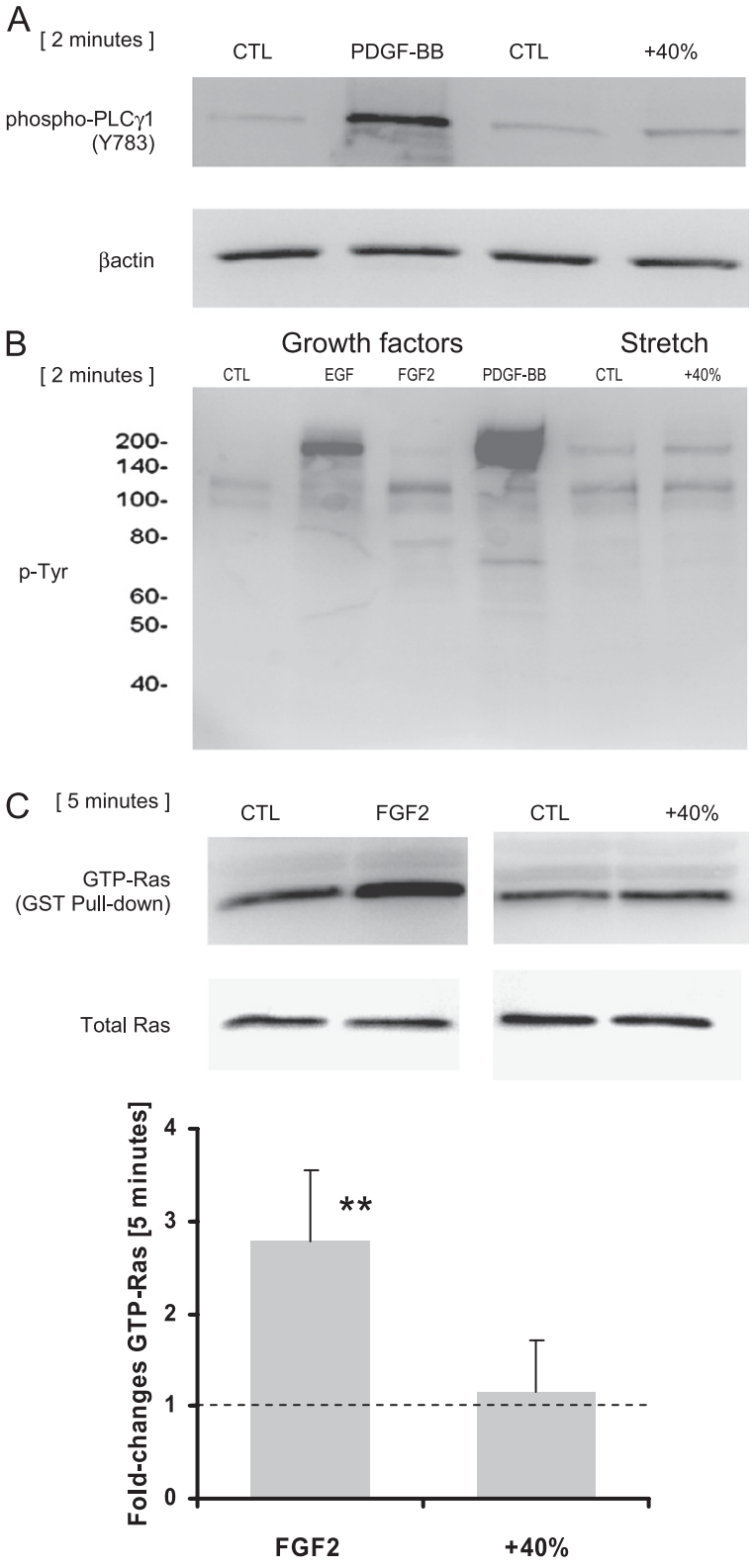

Figure 8. Indicators of RTK activation are not stimulated by stretch. (*A*) Phosphorylation of PLCγ1 is unchanged by stretch. CCL-151 cells were stimulated for 2 minutes by 100 ng/ml PDGF-BB or 40% tonic stretch. Wells were pooled as described in Figure 5, and tyrosine phosphorylation of PLCγ1 was analyzed by immunoblotting. Blots shown are representative of similar results in two independent experiments. (*B*) Phosphotyrosine levels unaltered by stretch. Ligands for EGFR, FGFR, and PDGFR or 40% stretch were applied for 2 minutes to CCL-151 cells grown in separate 6-well plates. Cell lysates were collected, pooled, and resolved by electrophoresis. Proteins above 30 kD molecular weight were transferred to membranes and probed with antiphospho-tyrosine antibody. (*C*) Stretch does not activate Ras. FGF2 (100 ng/mL) or 40% stretch were applied for 5 minutes to CCL-151 cells. Cell lysates were pooled and analyzed for Ras activation. (*Top*) A representative GTP-Ras pull-down blot and total Ras content is shown. (*Bottom*) Fold increase of GTP-Ras content was computed by dividing treated by time-matched untreated (CTL = control). Data are from three independent experiments.

cluding cell-surface mechanoreceptors such as integrins, dystroglycan, G protein–coupled receptors, and Ca^{2+}–permeable channels (e.g., the transient receptor potential and stretch-activated channels) (12, 13, 52–54). Alternatively, stretch could be transduced through intracellular mechanosensors such as p130cas (55) or through a protruding cell structure like the primary cilium.

Taken together, our findings demonstrate that human LFs are strongly responsive to stretch and exhibit polarity in stretch responsiveness, suggesting they are poised to play selective roles in lung growth and remodeling responses to stretch. Even though RTKs have been broadly implicated in lung mechanotransduction, our results reveal that they do not participate in proximal stretch-induced MAPK activation in lung fibroblasts.

Given the potent role that mechanical stretch plays in lung development and compensatory growth, further elucidation of the pathways and mechanotransducers involved in stretch-induced fibroblast signaling may give us new insights into how stretch promotes lung growth and regeneration.

Conflict of Interest Statement: None of the authors has a financial relationship with a commercial entity that has an interest in the subject of this manuscript.

References

1. Unbekandt M, del Moral PM, Sala FG, Bellusci S, Warburton D, Fleury V. Tracheal occlusion increases the rate of epithelial branching of embryonic mouse lung via the fgf10-fgfr2b-sprouty2 pathway. *Mech Dev* 2008;125:314–324.
2. Hooper SB, Han VK, Harding R. Changes in lung expansion alter pulmonary DNA synthesis and igf-ii gene expression in fetal sheep. *Am J Physiol* 1993;265:L403–L409.
3. Khan PA, Cloutier M, Piedboeuf B. Tracheal occlusion: a review of obstructing fetal lungs to make them grow and mature. *Am J Med Genet C Semin Med Genet* 2007;145C:125–138.
4. Cohn R. Factors affecting the postnatal growth of the lung. *Anat Rec* 1939;75:195–205.
5. Hsia CC. Signals and mechanisms of compensatory lung growth. *J Appl Physiol* 2004;97:1992–1998.
6. Ravikumar P, Yilmaz C, Dane DM, Johnson RL Jr, Estrera AS, Hsia CC. Regional lung growth following pneumonectomy assessed by computed tomography. *J Appl Physiol* 2004;97:1567–1574, discussion 1549.
7. Nardo L, Maritz G, Harding R, Hooper SB. Changes in lung structure and cellular division induced by tracheal obstruction in fetal sheep. *Exp Lung Res* 2000;26:105–119.
8. Seaborn T, St-Amand J, Cloutier M, Tremblay MG, Maltais F, Dinel S, Moulin V, Khan PA, Piedboeuf B. Identification of cellular processes that are rapidly modulated in response to tracheal occlusion within mice lungs. *Pediatr Res* 2008;63:124–130.
9. Pearson G, Robinson F, Beers Gibson T, Xu BE, Karandikar M, Berman K, Cobb MH. Mitogen-activated protein (map) kinase pathways: regulation and physiological functions. *Endocr Rev* 2001; 22:153–183.
10. Kyriakis JM, Avruch J. Mammalian mitogen-activated protein kinase signal transduction pathways activated by stress and inflammation. *Physiol Rev* 2001;81:807–869.
11. Chang L, Karin M. Mammalian map kinase signalling cascades. *Nature* 2001;410:37–40.
12. Wang JH, Thampatty BP. An introductory review of cell mechanobiology. *Biomech Model Mechanobiol* 2006;5:1–16.
13. Orr AW, Helmke BP, Blackman BR, Schwartz MA. Mechanisms of mechanotransduction. *Dev Cell* 2006;10:11–20.
14. Robinson DR, Wu YM, Lin SF. The protein tyrosine kinase family of the human genome. *Oncogene* 2000;19:5548–5557.
15. Liu M, Liu J, Buch S, Tanswell AK, Post M. Antisense oligonucleotides for pdgf-b and its receptor inhibit mechanical strain-induced fetal lung cell growth. *Am J Physiol* 1995;269:L178–L184.
16. Sanchez-Esteban J, Wang Y, Gruppuso PA, Rubin LP. Mechanical stretch induces fetal type ii cell differentiation via an epidermal growth factor receptor-extracellular-regulated protein kinase signaling pathway. *Am J Respir Cell Mol Biol* 2004;30:76–83.
17. Correa-Meyer E, Pesce L, Guerrero C, Sznajder JI. Cyclic stretch activates erk1/2 via g proteins and EGFR in alveolar epithelial cells. *Am J Physiol Lung Cell Mol Physiol* 2002;282:L883–L891.
18. Kippenberger S, Loitsch S, Guschel M, Muller J, Knies Y, Kaufmann R, Bernd A. Mechanical stretch stimulates protein kinase b/akt phosphorylation in epidermal cells via angiotensin ii type 1 receptor and epidermal growth factor receptor. *J Biol Chem* 2005;280:3060–3067.
19. Cheng J, Du J. Mechanical stretch simulates proliferation of venous smooth muscle cells through activation of the insulin-like growth factor-1 receptor. *Arterioscler Thromb Vasc Biol* 2007;27:1744–1751.
20. Iwasaki H, Eguchi S, Ueno H, Marumo F, Hirata Y. Mechanical stretch stimulates growth of vascular smooth muscle cells via epidermal growth factor receptor. *Am J Physiol Heart Circ Physiol* 2000;278: H521–H529.
21. Hu Y, Bock G, Wick G, Xu Q. Activation of pdgf receptor alpha in vascular smooth muscle cells by mechanical stress. *FASEB J* 1998;12: 1135–1142.
22. Wilson E, Mai Q, Sudhir K, Weiss RH, Ives HE. Mechanical strain induces growth of vascular smooth muscle cells via autocrine action of pdgf. *J Cell Biol* 1993;123:741–747.
23. Shimizu N, Yamamoto K, Obi S, Kumagaya S, Masumura T, Shimano Y, Naruse K, Yamashita JK, Igarashi T, Ando J. Cyclic strain induces mouse embryonic stem cell differentiation into vascular smooth muscle cells by activating pdgf receptor beta. *J Appl Physiol* 2008; 104:766–772.
24. Putnam AJ, Cunningham JJ, Dennis RG, Linderman JJ, Mooney DJ. Microtubule assembly is regulated by externally applied strain in cultured smooth muscle cells. *J Cell Sci* 1998;111:3379–3387.
25. Powers CJ, McLeskey SW, Wellstein A. Fibroblast growth factors, their receptors and signaling. *Endocr Relat Cancer* 2000;7:165–197.
26. Leahy DJ. Structure and function of the epidermal growth factor (egf/erbb) family of receptors. *Adv Protein Chem* 2004;68:1–27.
27. Westermark B, Claesson-Welsh L, Heldin CH. Structural and functional aspects of platelet-derived growth factor and its receptors. *Ciba Found Symp* 1990;150:6–14, discussion 14–22.
28. Fujioka A, Terai K, Itoh RE, Aoki K, Nakamura T, Kuroda S, Nishida E, Matsuda M. Dynamics of the ras/erk mapk cascade as monitored by fluorescent probes. *J Biol Chem* 2006;281:8917–8926.
29. Moon SK, Cha BY, Kim CH. Erk1/2 mediates tnf-alpha-induced matrix metalloproteinase-9 expression in human vascular smooth muscle cells via the regulation of nf-kappab and ap-1: involvement of the ras dependent pathway. *J Cell Physiol* 2004;198:417–427.
30. Sneddon WB, Yang Y, Ba J, Harinstein LM, Friedman PA. Extracellular signal-regulated kinase activation by parathyroid hormone in distal tubule cells. *Am J Physiol Renal Physiol* 2007;292:F1028–F1034.
31. Moriguchi T, Toyoshima F, Gotoh Y, Iwamatsu A, Irie K, Mori E, Kuroyanagi N, Hagiwara M, Matsumoto K, Nishida E. Purification and identification of a major activator for p38 from osmotically shocked cells: activation of mitogen-activated protein kinase kinase 6 by osmotic shock, tumor necrosis factor-alpha, and h2o2. *J Biol Chem* 1996;271:26981–26988.
32. Kito H, Chen EL, Wang X, Ikeda M, Azuma N, Nakajima N, Gahtan V, Sumpio BE. Role of mitogen-activated protein kinases in pulmonary endothelial cells exposed to cyclic strain. *J Appl Physiol* 2000;89: 2391–2400.
33. Park CH, Lee MJ, Ahn J, Kim S, Kim HH, Kim KH, Eun HC, Chung JH. Heat shock-induced matrix metalloproteinase (mmp)-1 and mmp-3 are mediated through erk and jnk activation and via an autocrine interleukin-6 loop. *J Invest Dermatol* 2004;123:1012–1019.
34. Cao C, Lu S, Jiang Q, Wang WJ, Song X, Kivlin R, Wallin B, Bagdasarian A, Tamakloe T, Chu WM, *et al.* Egfr activation confers protections against uv-induced apoptosis in cultured mouse skin dendritic cells. *Cell Signal* 2008;20:1830–1838.
35. Tacheau C, Fontaine J, Loy J, Mauviel A, Verrecchia F. Tgf-beta induces connexin43 gene expression in normal murine mammary gland epithelial cells via activation of p38 and pi3k/akt signaling pathways. *J Cell Physiol* 2008;217:759–768.
36. The Acute Respiratory Distress Syndrome Network. Ventilation with lower tidal volumes as compared with traditional tidal volumes for acute lung injury and the acute respiratory distress syndrome. *N Engl J Med* 2000;342:1301–1308.
37. Tschumperlin DJ, Oswari J, Margulies AS. Deformation-induced injury of alveolar epithelial cells: effect of frequency, duration, and amplitude. *Am J Respir Crit Care Med* 2000;162:357–362.
38. Tschumperlin DJ, Margulies SS. Alveolar epithelial surface area-volume relationship in isolated rat lungs. *J Appl Physiol* 1999;86: 2026–2033.
39. Eswarakumar VP, Lax I, Schlessinger J. Cellular signaling by fibroblast growth factor receptors. *Cytokine Growth Factor Rev* 2005;16: 139–149.
40. Cartel NJ, Liu J, Wang J, Post M. Pdgf-bb-mediated activation of p42(mapk) is independent of pdgf beta-receptor tyrosine phosphorylation. *Am J Physiol Lung Cell Mol Physiol* 2001;281:L786–L798.
41. Wiley HS. Trafficking of the erbb receptors and its influence on signaling. *Exp Cell Res* 2003;284:78–88.
42. Rosette C, Karin M. Ultraviolet light and osmotic stress: activation of the jnk cascade through multiple growth factor and cytokine receptors. *Science* 1996;274:1194–1197.
43. Liu M, Qin Y, Liu J, Tanswell AK, Post M. Mechanical strain induces pp60src activation and translocation to cytoskeleton in fetal rat lung cells. *J Biol Chem* 1996;271:7066–7071.

44. Bromann PA, Korkaya H, Courtneidge SA. The interplay between src family kinases and receptor tyrosine kinases. *Oncogene* 2004;23:7957–7968.
45. Vaccaro C, Brody JS. Ultrastructure of developing alveoli. I: the role of the interstitial fibroblast. *Anat Rec* 1978;192:467–479.
46. Rebecchi MJ, Pentyala SN. Structure, function, and control of phosphoinositide-specific phospholipase c. *Physiol Rev* 2000;80: 1291–1335.
47. Rhee SG. Regulation of phosphoinositide-specific phospholipase c. *Annu Rev Biochem* 2001;70:281–312.
48. Takai Y, Sasaki T, Matozaki T. Small gtp-binding proteins. *Physiol Rev* 2001;81:153–208.
49. Prenzel N, Zwick E, Daub H, Leserer M, Abraham R, Wallasch C, Ullrich A. Egf receptor transactivation by g-protein-coupled receptors requires metalloproteinase cleavage of prohb-egf. *Nature* 1999; 402:884–888.
50. Fischer OM, Hart S, Gschwind A, Prenzel N, Ullrich A. Oxidative and osmotic stress signaling in tumor cells is mediated by adam proteases and heparin-binding epidermal growth factor. *Mol Cell Biol* 2004;24: 5172–5183.
51. Sundberg C, Rubin K. Stimulation of beta1 integrins on fibroblasts induces pdgf independent tyrosine phosphorylation of pdgf beta-receptors. *J Cell Biol* 1996;132:741–752.
52. Ingber DE. Cellular mechanotransduction: putting all the pieces together again. *FASEB J* 2006;20:811–827.
53. Jones JC, Lane K, Hopkinson SB, Lecuona E, Geiger RC, Dean DA, Correa-Meyer E, Gonzales M, Campbell K, Sznajder JI, *et al.* Laminin-6 assembles into multimolecular fibrillar complexes with perlecan and participates in mechanical-signal transduction via a dystroglycan-dependent, integrin-independent mechanism. *J Cell Sci* 2005;118:2557–2566.
54. Ito S, Kume H, Naruse K, Kondo M, Takeda N, Iwata S, Hasegawa Y, Sokabe M. A novel Ca2+ influx pathway activated by mechanical stretch in human airway smooth muscle cells. *Am J Respir Cell Mol Biol* 2008;38:407–413.
55. Sawada Y, Tamada M, Dubin-Thaler BJ, Cherniavskaya O, Sakai R, Tanaka S, Sheetz MP. Force sensing by mechanical extension of the src family kinase substrate p130cas. *Cell* 2006;127:1015–1026.